RAA 2018 Vol. **18** No. **3**, 29(10pp) doi: 10.1088/1674–4527/18/3/29

http://www.raa-journal.org *http://iopscience.iop.org/raa*

***R**esearch in*
***A**stronomy and*
***A**strophysics*

Anisotropic power spectrum and the observed low-l power in PLANCK CMB data

Zhe Chang[1,2], Pranati K. Rath[1,3], Yu Sang[1,2] and Dong Zhao[1,2]

[1] Institute of High Energy Physics, Chinese Academy of Sciences, Beijing 100049, China
[2] University of Chinese Academy of Sciences, Beijing 100049, China
[3] Theoretical Physics Center for Science Facilities, Chinese Academy of Sciences, Beijing 100049, China; *pranati@ihep.ac.cn*

Received 2017 October 13; accepted 2017 December 17

Abstract In this work, we study a direction dependent power spectrum in anisotropic Finsler space-time. We use this direction dependent power spectrum to address the low-l power observed in WMAP and PLANCK data. The angular power spectrum of the temperature fluctuations has a lower amplitude in comparison to the ΛCDM model in the multipole range $l = 2 - 40$. Our theoretical model gives a correction to the isotropic angular power spectrum C_l^{TT} due to the breaking of rotational invariance of the primordial power spectrum. We estimate best-fit model parameters along with the six ΛCDM cosmological parameters using the PLANCK likelihood code in CosmoMC software. We find that this modified angular power spectrum fits the CMB temperature data in the multipole range $l = 2 - 10$ to a good extent but fails for the whole multipole range $l = 2 - 40$.

Key words: cosmic background radiation — large-scale structure of universe

1 INTRODUCTION

The standard Lambda cold dark matter (ΛCDM) cosmological model predicted by the inflationary scenario in the very early Universe is impressively successful in explaining the observed Cosmic Microwave Background (CMB) data. However, a set of CMB observations which is not statistically consistent with the ΛCDM model has been observed in both WMAP and PLANCK CMB data. These observations include alignment of CMB quadrupole and octopole (de Oliveira-Costa et al. 2004; Copi et al. 2004; Ralston & Jain 2004; Land & Magueijo 2005; Abramo et al. 2006b,a; Copi et al. 2015b), lack of power at large scale up to $l \leq 40$ (Jing & Fang 1994; Bennett et al. 2011; Planck Collaboration et al. 2014a; Iqbal et al. 2015), the lack of large angular correlations on angular scales larger than 60° (Spergel et al. 2003; Copi et al. 2009, 2015a) and hemispherical power asymmetry (Eriksen et al. 2004, 2007; Erickcek et al. 2008b,a; Hansen et al. 2009; Hanson & Lewis 2009; Groeneboom et al. 2010; Hoftuft et al. 2009; Planck Collaboration et al. 2016b; Rath & Jain 2013; Rath et al. 2015; Jain & Rath 2015). The CMB observations also suggest parity asymmetry (Kim & Naselsky 2010a,b; Gruppuso et al. 2011; Kim & Naselsky 2011; Aluri & Jain 2012; Ben-David et al. 2012; Zhao 2014; Shiraishi et al. 2015; Aluri et al. 2017) and a cold spot in the southern hemisphere (Cruz et al. 2005, 2006, 2008; Vielva 2010; Lim & Simon 2012). The significance of these observations has motivated many theorists to study different theoretical models. Hence there exists a number of theoretical models based on anisotropic space-times (Berera et al. 2004; Kahniashvili et al. 2008; Ackerman et al. 2007; Chang & Wang 2013) and an inhomogeneous Universe (Moffat 2005). The theoretical models violating rotational invariance lead to a direction dependency in the primordial power spectrum (Ackerman et al. 2007; Goldwirth & Piran 1990; Emir Gümrükçüoglu et al. 2007; Pontzen & Challinor 2007; Pereira et al. 2007; Pullen & Kamionkowski 2007; Campanelli 2009;

Donoghue et al. 2009; Watanabe et al. 2009; Chang & Wang 2013).

The primordial power spectrum $P(k)$, defined as the two-point correlation function of the primordial density perturbation $\delta(\boldsymbol{k})$, can be written as

$$\langle \delta(\boldsymbol{k})\delta^*(\boldsymbol{k}')\rangle = (2\pi)^3\delta^3(\boldsymbol{k}-\boldsymbol{k}')P(k)\,. \tag{1}$$

The Dirac delta function in Equation (1) ensures that the modes with different wave numbers are not coupled with each other, which is the consequence of translational invariance. In the standard ΛCDM model which refers to the homogeneous and isotropic Friedmann-Robertson-Walker (FRW) metric, fluctuations are statistically isotropic and the primordial power spectrum $P(k)$ depends only on the magnitude of the wave vector $\boldsymbol{k}$. Hence the primordial power spectrum is rotationally invariant and one can write the primordial power spectrum $P(k)$ as

$$P(k) = A_s\left(\frac{k}{k_c}\right)^{n_s-1}, \tag{2}$$

where n_s is the spectral index, A_s is the spectral amplitude and k_c is the scalar pivot. In this case, the spherical harmonic coefficient a^T_{lm} of the temperature fluctuation obeys statistical isotropy and hence the two-point correlation of a^T_{lm} can be written as

$$\left\langle a^T_{lm}a^{T*}_{l'm'}\right\rangle = C^{TT}_l\delta_{ll'}\delta_{mm'}, \tag{3}$$

where C^{TT}_l is the angular power spectrum encoding all the information about CMB temperature fluctuations.

But in case of an anisotropic space-time which breaks rotational invariance of the power spectrum, the spherical harmonic coefficient a^T_{lm} no longer follows statistical isotropy and the two-point correlation function of a^T_{lm} gives rise to off-diagonal correlation between multipole moments. The off-diagonal correlations encode all the crucial information regarding the anisotropic model. Hence one can write

$$\left\langle a^T_{lm}a^{T*}_{l'm'}\right\rangle \equiv C^{TT}_{ll'mm'}. \tag{4}$$

In WMAP and PLANCK data, it has been observed that the temperature angular power spectrum, C^{TT}_l, at low-l ($l \leq 40$) has a lower amplitude than the ΛCDM model (Bennett et al. 2011; Planck Collaboration et al. 2014b,a, 2016a). In Hazra et al. (2014), the authors also studied consistency of the ΛCDM model with the PLANCK data and claimed that the data have a lack of power at both high and low l multipoles. This issue has been studied extensively by many theorists in the inflationary framework (Contaldi et al. 2003; Boyanovsky et al. 2006; Cicoli et al. 2014; Das & Souradeep 2014). In this paper, we try to relate the direction dependent power spectrum with the lack of power at large scale and find the best-fit model parameters.

The paper is organized as follows. In Section 2, we review briefly Finsler space-time and a direction dependent power spectrum in this space-time. Then, in Section 3, we implement this power spectrum to study the lack of power at large scale. To study its effect on the angular power spectrum C^{TT}_l, we perform Markov Chain Monte Carlo (MCMC) analysis using PLANCK data. In Section 4, we present results of the MCMC analysis. In Section 5, we summarize our work.

2 ANISOTROPIC MODEL

Here we briefly review an anisotropic space-time in the framework of Finsler geometry (Chang & Li 2009; Chang et al. 2013; Chang & Wang 2013; Li et al. 2015b). Chang & Wang (2013); Li et al. (2015b) studied anisotropic inflation taking Finslerian background spacetime. Finsler spacetime has fewer symmetries than Riemann symmetry and hence is a suitable candidate to study the anisotropy observations. The counterparts of special relativity (Gibbons et al. 2007; Chang & Li 2008; Chang & Wang 2012), commonly known as very special relativity (Coleman & Glashow 1997, 1999; Cohen & Glashow 2006), have connections with Finsler geometry (Bao et al. 2012), which is generalized from Riemann geometry by removing the quadratic restriction. In order to investigate these counterparts, one should study the inertial frames and symmetry in Finsler spacetime. The symmetry of spacetime is described by investigating the Killing vectors (Li & Chang 2012). Finsler geometry is defined on the tangent bundle with proper length, s, as

$$s = \int_a^b F(x,y)ds\,, \tag{5}$$

where x and $y \equiv dx/ds$ are the position and velocity respectively. The integrand $F(x,y)$, which is known as the Finsler structure, is the basis of Finsler geometry. This is a smooth and positive function on the tangent bundle of a manifold M. For any $\lambda > 0$, Finsler structure F obeys

$$F(x,\lambda y) = \lambda F(x,y)\,. \tag{6}$$

The Finsler metric is given by the second derivative of F^2 with respect to velocity y as

$$g_{\mu\nu} = \frac{\partial}{\partial y^\mu}\frac{\partial}{\partial y^\nu}\left(\frac{1}{2}F^2\right), \quad (7)$$

where the spatial indices of μ and ν run from 1 to 3 and the temporal index is 0. A Finsler metric is said to be locally Minkowskian if at every point there exists a local coordinate system in which the Finsler structure F is independent of the position x, i.e, $F = F(y)$. This is known as flat Finsler space-time. Flat Finsler space-time can be used to test Lorentz invariance through the modified dispersion relation. The geodesic equations in Finsler space-time can be given by the first order variation of Finslerian length as (Li & Lin 2017)

$$\frac{d^2x^\mu}{d\tau^2} + 2G^\mu = 0, \quad (8)$$

where the geodesic spray coefficient G^μ is defined as

$$G^\mu = \frac{1}{4}g^{\mu\nu}\left(\frac{\partial^2F^2}{\partial x^\lambda \partial y^\nu}y^\lambda - \frac{\partial F^2}{\partial x^\nu}\right). \quad (9)$$

The coefficient G^μ vanishes in the local Minkowski space.

The observed CMB anomalies may be related to a special case of Finsler space-time known as Randers-Finsler space-time. Randers space (Randers 1941) involves a vector field which may influence the anisotropic evolution of the early Universe. The structure is given by

$$F^2 = y^t y^t - a^2(t)F_{Ra}^2\,. \quad (10)$$

Here F_{Ra}^2 is the structure of Randers space, and

$$F_{Ra}^2(x,y) = \alpha(x,y) + \beta(x,y)\,, \quad (11)$$

where $\alpha(x,y) = \sqrt{\tilde{a}_{\mu\nu}(x)y^\mu y^\nu}$ is a Riemann structure with metric $\tilde{a}_{\mu\nu}$, and $\beta(x,y) = \tilde{b}_\mu(x)y^\mu$ is a 1-form. This vector induces the anisotropic properties in the Randers space. Here, $\tilde{a}_{\mu\nu}$ can be taken as the flat FRW metric, and $\tilde{b}_\mu$ has only the temporal component, i.e., $\tilde{b}_\mu = (B(z), 0, 0, 0)$, where $B(z)$ depends on the third spatial coordinate z. The Finsler metric will be reduced to the FRW metric if $B(z) \to 0$. The 1-form $\beta(x,y)$ is relevant to a vector field, which will give a privileged axis in the space-time.

To investigate the Killing vector, one should discuss the isometric transformation under an infinitesimal coordinate transformation. The isometric transformations for x and y are defined by

$$\bar{x}^\mu = x^\mu + \epsilon V^\mu, \quad (12)$$

$$\bar{y}^\mu = y^\mu + \epsilon\frac{\partial V^\mu}{\partial x^\nu}y^\nu. \quad (13)$$

In the first order of ϵ, the Finsler structure is

$$\bar{F}(\bar{x},\bar{y}) = \bar{F}(x,y) + \epsilon V^\mu\frac{\partial F}{\partial x^\mu} + \epsilon y^\nu\frac{\partial V^\mu}{\partial x^\nu}\frac{\partial F}{\partial y^\mu}\,. \quad (14)$$

The Finsler structure is called isometric if and only if $F(x,y) = \bar{F}(x,y)$. Hence one can obtain the Killing equation in Finsler space as

$$K_V(F) \equiv V^\mu\frac{\partial F}{\partial x^\mu} + y^\nu\frac{\partial V^\mu}{\partial x^\nu}\frac{\partial F}{\partial x^\mu} = 0\,. \quad (15)$$

Using Equation (11), one can see that the number of independent Killing vectors in Randers-Finsler space-time is less than that in Riemannian space-time.

The speed of light is direction dependent in Finsler space-time. Along the radial direction, it can be derived as (Li & Chang 2010, 2014; Li et al. 2015a)

$$c_r = \frac{1}{1 + B\cos\theta}\,, \quad (16)$$

where θ is the angle along the z-axis. Hence the redshift in Finsler space-time is

$$1 + z = \frac{1 + B\cos\theta}{a}. \quad (17)$$

The variation in speed of light from Equation (16) yields a variation of the fine-structure constant, which is a dipolar distribution. This dipolar distribution of the fine structure constant agrees with observations of quasar absorption spectra (Webb et al. 2011; King et al. 2012; Chang et al. 2012). Using Equation (17), the luminosity distance in a Finslerian Universe is stated as

$$d_L = (1+z)r = \frac{1+z}{H_0}\int_0^z \frac{dz}{\sqrt{\Omega_{m0}(1+z)^3(1 - 3B\cos\theta) + 1 - \Omega_{m0}}}\,, \quad (18)$$

where the radial distance $r = \sqrt{x^2 + y^2 + z^2}$.

In the standard cosmological model, the power spectrum is derived in isotropic space-time. However, if there exists a privileged direction in space-time, the early evolution of the Universe will have different behaviors. This anisotropic space-time at the early stage of inflation breaks the rotational invariance of the primordial power spectrum and leads to a direction dependent power spectrum. Taking Randers space-time with a weak vector field, i.e., $|\tilde{b}_\mu| \ll 1$, as the background space-time of inflation and solving the equation of motion of the inflaton field, one can obtain a direction dependent power spectrum of the form

$$P'(k) = P_{\rm iso}(k)\left(1 + iA(k)\left(\hat{k}\cdot\hat{n}\right) + B(k)\left(\hat{k}\cdot\hat{n}\right)^2\right), \quad (19)$$

where $P_{\rm iso}(k)$ denotes the isotropic power spectrum, and $A(k)$ and $B(k)$ are some arbitrary functions of wave number k. The functions $A(k)$ and $B(k)$ encode the amplitude of dipolar and quadrupolar modulation to the isotropic power spectrum respectively. We restrict ourselves to the second order correction of the isotropic primordial power spectrum as the next higher order terms in $(\hat{k}\cdot\hat{n})$ will be suppressed by the magnitude of the small vector. The breaking of rotational invariance of the primordial power spectrum leads to non-vanishing correlations between different multipole moments that would normally vanish. The same type of direction dependent power spectrum in the leading order of $(\hat{k}\cdot\hat{n})$ was obtained in Rath et al. (2015); Jain & Rath (2015); Kothari et al. (2016); Ghosh et al. (2016); Zibin & Contreras (2017); Chang & Wang (2013); Li et al. (2015b) to address the hemispherical power asymmetry successfully. Rath et al. (2015); Jain & Rath (2015); Kothari et al. (2016); Ghosh et al. (2016) constrained the amplitude in the multipole range $l=2-64$ with a 3σ confidence level using PLANCK data. The amplitude for the quadrupolar modulation $B(k)$ has been constrained by Kim & Komatsu (2013); Planck Collaboration et al. (2016c) and they found it to be an order of 10^{-2}. Here we do not give any remark on the quadrupolar modulation constraint and focus only on the correction to the isotropic power spectrum due to the quadrupolar modulation in the power spectrum.

3 APPLICATION TO CMB DATA

The temperature fluctuation in terms of primordial density fluctuations $\delta(k)$ can be written as

$$\frac{\Delta T}{T_0}(\hat{n}) = \int d^3k \sum_l \frac{2l+1}{4\pi}(-i)^l P_l(\hat{k}\cdot\hat{n})\delta(k)\Delta_l^T(k)\,, \tag{20}$$

where P_l and $\Delta_l^T(k)$ are the Legendre polynomial and the transfer function of order l respectively. The transfer function helps in understanding the change in amplitude of the perturbation from an initial time to the current time. Now using Equation (20) one can write the spherical harmonic coefficients a_{lm}^T as

$$a_{lm}^T = \int d\Omega Y_{lm}^*(\hat{n})\Delta T(\hat{n})\,, \tag{21}$$

and the two-point correlation function of a_{lm}^T as

$$\langle a_{lm}^T a_{l'm'}^{T*}\rangle = \langle a_{lm}^T a_{l'm'}^{T*}\rangle_{\rm iso} + \langle a_{lm}^T a_{l'm'}^{T*}\rangle_{\rm aniso}\,, \tag{22}$$

where the first term gives the isotropic angular power spectrum C_l^{TT}

$$C_l^{TT} = \int_0^\infty k^2 dk P_{\rm iso}(k)(\Delta_l^T(k))^2\,, \tag{23}$$

and the second term contains all the anisotropic terms. Following Equation (4), one can write the anisotropic term as

$$C_{ll'mm'}^{TT} = \langle a_{lm}a_{l'm'}^*\rangle_{dm} + \langle a_{lm}a_{l'm'}^*\rangle_{qm}\,, \tag{24}$$

where the dipole modulation term is given as

$$\langle a_{lm}a_{l'm'}^*\rangle_{dm} = (-i)^{l-l'}\xi_{lm;l'm'}^{dm}\int_0^\infty k^2 dk\, P_{\rm iso}(k)A(k)\Delta_l^T(k)\Delta_{l'}^T(k)\,, \tag{25}$$

and the quadrupolar modulation term is given as

$$\langle a_{lm}a_{l'm'}^*\rangle_{qm} = (-i)^{l-l'}\xi_{lm;l'm'}^{qm}\int_0^\infty k^2 dk\, P_{\rm iso}(k)B(k)\Delta_l^T(k)\Delta_{l'}^T(k)\,. \tag{26}$$

Following Ackerman et al. (2007); Rath et al. (2013), we use the spherical components of the unit vector n as

$$\begin{aligned} n_+ &= -\left(\frac{n_x - in_y}{\sqrt{2}}\right),\\ n_- &= \left(\frac{n_x + in_y}{\sqrt{2}}\right),\\ n_0 &= n_z\,. \end{aligned} \tag{27}$$

The geometrical factor $\xi_{lm;l'm'}^{dm}$ of the dipolar modulation term is defined as

$$\xi_{lm;l'm'}^{dm} = n_+\xi_{lm;l'm'}^{dm+} + n_-\xi_{lm;l'm'}^{dm-} + n_0\xi_{lm;l'm'}^{dm0}\,, \tag{28}$$

which gives the correlation between multipole moments that differ by $\Delta l = 1$ and it has no effect on the isotropic angular power spectrum C_l^{TT}. Hence by making the preferred axis the z-axis, the coefficients of $\xi_{lm;l'm'}^{dm}$ can be given as

$$\xi_{lm;l'm'}^{dm0} = \delta_{m',m}\left[\sqrt{\frac{(l-m+1)(l+m+1)}{(2l+1)(2l+3)}}\delta_{l',l+1} + \sqrt{\frac{(l-m)(l+m)}{(2l+1)(2l-1)}}\delta_{l',l-1}\right]. \tag{29}$$

This term successfully explains the observed hemispherical power asymmetry (Rath et al. 2015; Kothari et al. 2016; Ghosh et al. 2016; Chang & Wang 2013; Li et al. 2015b).

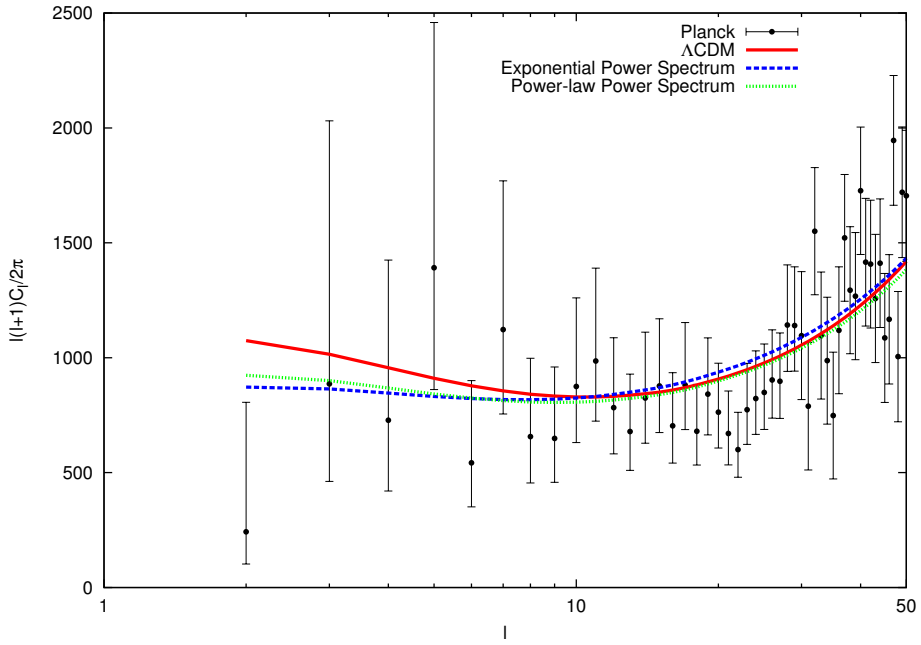

Fig. 1 Points with error bars represent the PLANCK 2015 temperature power spectrum for $l = 2 - 50$. The red solid line stands for the ΛCDM power spectrum and the green-dotted line traces the theoretical power spectrum for the power law case with best-fit parameters $(B_0, \alpha) = (0.04, 0.4556 \pm 0.2158)$. The blue-dotted line presents the theoretical power spectrum for the exponential form with best-fit parameters $(B_0, \alpha) = (0.4229 \pm 0.1134, 4.2889 \pm 1.2173)$.

Next, we will discuss the quadrupolar modulation term in the power spectrum. The geometrical factor $\xi^{qm}_{lm;l'm'}$ of the quadrupolar modulation term is given as

$$\begin{aligned}\xi^{qm}_{lm;l'm'} &= n_+^2 \xi^{qm++}_{lm;l'm'} + n_-^2 \xi^{qm--}_{lm;l'm'} \\ &+2n_+n_- \xi^{qm+-}_{lm;l'm'} + 2n_+n_0 \xi^{qm+0}_{lm;l'm'} \\ &+2n_-n_0 \xi^{qm-0}_{lm;l'm'} + n_0^2 \xi^{qm00}_{lm;l'm'} . \end{aligned} \quad (30)$$

This term contains all the correlations between multipoles that differ by $\Delta l = 2$ and $\Delta l = 0$. Hence the isotropic angular power spectrum C_l^{TT} changes if we consider the coefficients with $\Delta l = 0$. The coefficients of $\xi^{qm}_{lm;l'm'}$ for $l' = l$ and $m' = m$ are

$$\xi^{qm+-}_{lm;l'm'} = -\delta_{m',m} \frac{(l^2 + m^2 + l - 1)}{(2l-1)(2l+3)}, \quad (31)$$

$$\xi^{qm00}_{lm;l'm'} = \delta_{m,m'} \frac{(2l^2 + 2l - 2m^2 - 1)}{(2l-1)(2l+3)}. \quad (32)$$

By setting the preferred direction along the z-axis, only $\xi^{qm00}_{lm;l'm'}$ will contribute to C_l^{TT}. This correction depends on the anisotropic power spectrum $B(k)$. Hence to estimate its effect on C_l^{TT}, we parameterize the anisotropic power spectrum $B(k)$. We try two forms of the anisotropic power spectrum $B(k)$; the first one is a power law form and the second one is an exponential form. The power law form of the anisotropic power spectrum is given as

$$B(k) = -B_0 \left(\frac{k}{k_c} \right)^{-\alpha} \quad (33)$$

and the exponential form of the anisotropic power spectrum is expressed as

$$B(k) = B_0 \exp \left[- \left(\frac{k}{k_c} \right)^{\alpha} \right], \quad (34)$$

where B_0 and α are the amplitude and spectral index of the anisotropic term respectively. In the next section, we will use both forms of $B(k)$ and estimate the theoretical model parameters B_0 and α in addition to six cosmological parameters using CosmoMC software.

4 ANALYSIS AND RESULTS

For our analysis, we use the publicly available CosmoMC software (Lewis & Challinor 2002) which consists of Fortran and Python codes. CosmoMC uses the CAMB (Lewis et al. 2000) code to compute the theoretical angular power spectrum and relies on MCMC to generate the best-fit cosmological parameters. To obtain the best-fit parameters using likelihood, we use

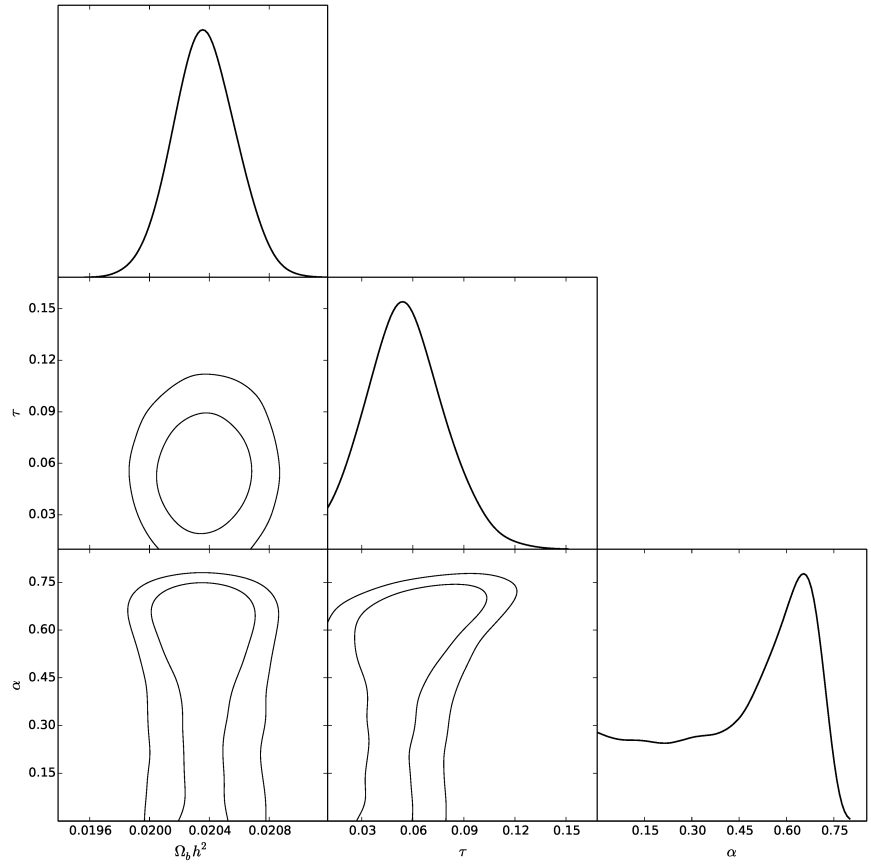

Fig. 2 The parameter plot for the power-law form of the anisotropic term in the power spectrum.

the PLANCK likelihood code (PLC/clik) provided by the PLANCK team with CosmoMC software (Planck Collaboration et al. 2014a). The PLANCK likelihood code uses COMMANDER at low-l ($l = 2 - 49$) and CamSpec code at high-l ($l = 50 - 2500$). The inputs to CosmoMC are the central values and the flat priors of the various model parameters. We execute CosmoMC's Python scripts and getdist to analyze the generated chains from the MCMC analysis and to produce the required plots.

We modify the required CAMB and CosmoMC code using Equation (19) for our analysis. We utilize Equations (33) and (34) for the anisotropic part of Equation (19). We apply flat priors for the model parameters B_0 and α in addition to the six ΛCDM parameters as input to the MCMC analysis. The parameters and their prior ranges are listed in Tables 1 and 2. We first check for the power law case of the anisotropic power spectrum in Equation (33) and then move to the exponential form in Equation (34). For the power law case, we first run for both the parameters and get a negative C_l error in the CosmoMC for some range of B_0 and α. The reason for getting negative C_l for those parameters is due to the larger value of the anisotropic term compared to the isotropic power spectrum. This is not acceptable at all. Hence we try by fixing one of these two parameters. We first fix α to different values and search for the best-fit value of B_0. In particular, by fixing α to 0.5, we find that the best-fit value of B_0 is 0.0342 ± 0.0396 which can explain the lack of power in low-l. But as we see the error in B_0 is larger than the best-fit value, we cannot use this result. So, we next try by fixing B_0 and allowing α to run in the range $[0, 0.8]$. We find that for $B_0 = 0.04$ and $\alpha = 0.4556 \pm 0.2158$, the theoretical model is able to explain the lack of power up to $l = 10$ to a good extent. This fitting is not as good as we want. Nonetheless, we list all the best-fit parameters in Table 3.

Next, we consider the exponential form of the anisotropic power spectrum. In this case, we allow both the model parameters to vary. We choose to run the parameters in the range $\alpha = [0, 8]$ and $B_0 = [-1, 1]$. By searching for the best-fit value in the chosen wide range,

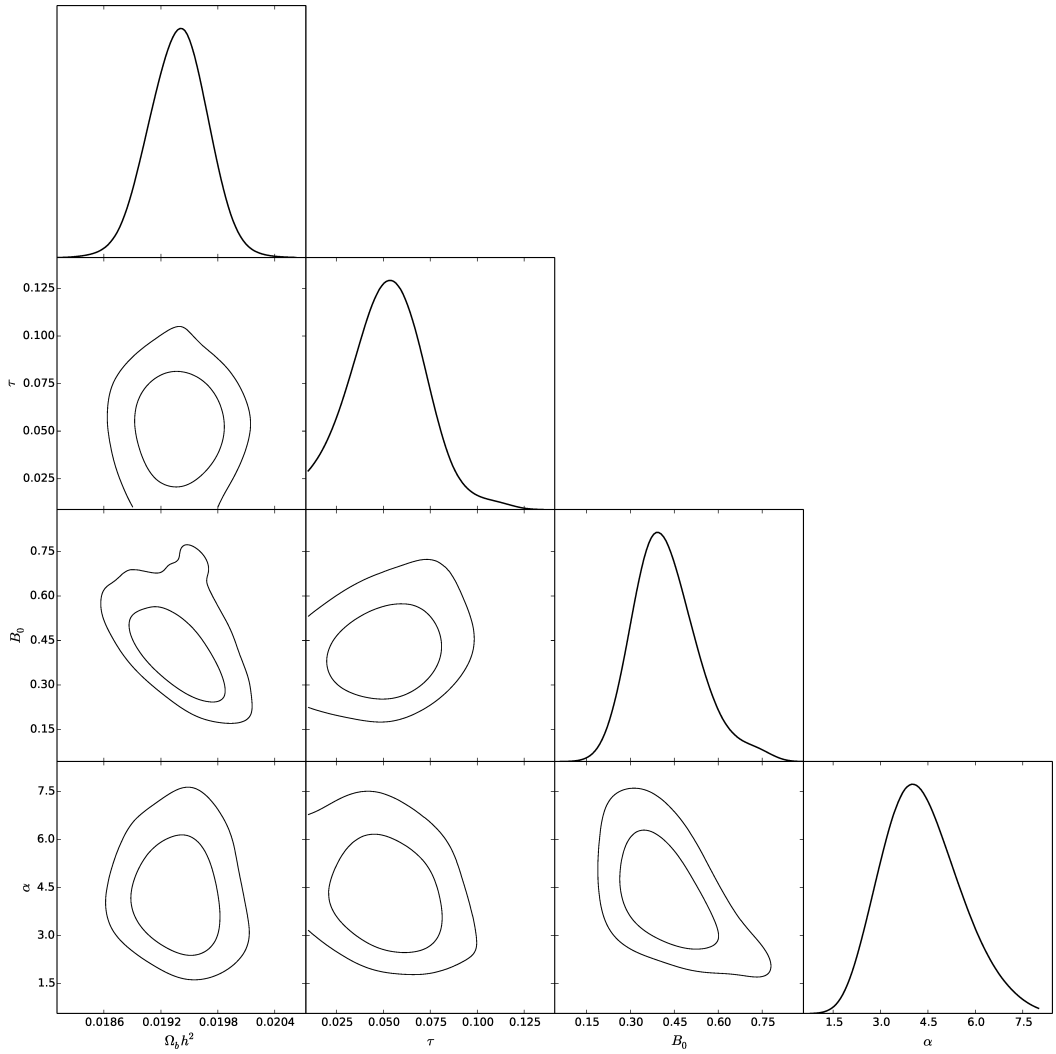

Fig. 3 The parameter plot for the exponential form of the anisotropic term in the power spectrum.

Table 1 Prior Range Used in Parameter Estimation Analysis for the Power Law Form

Parameter Name	Symbol	Prior Range
Baryon Density	$\Omega_b h^2$	[0.005, 0.1]
Cold Dark Matter Density	$\Omega_c h^2$	[0.001, 0.99]
Angular Size of Acoustic Horizon	$100\theta_{\rm MC}$	[0.5, 10.0]
Optical Depth	τ	[0.01, 0.8]
Scalar Spectral Index	n_s	[0.8, 1.2]
Scalar Amplitude	$\ln(10^{10} A_s)$	[2, 4]
Anisotropic Spectral Index	α	[0, 0.8]
Anisotropic Amplitude	B_0	0.04

we find the best-fit values as $\alpha = 4.2889 \pm 1.2173$ and $B_0 = 0.4229 \pm 0.1134$. The best-fit parameter values from the MCMC analysis are given in Table 3.

In Figure 1, we plot the PLANCK 2015 temperature power spectrum along with the best-fit theoretical power spectrum obtained from ΛCDM and from our theoretical model. In this figure, the power law and expo-

Table 2 Prior Range Used in Parameter Estimation Analysis for the Exponential Form

Parameter Name	Symbol	Prior Range
Baryon Density	$\Omega_b h^2$	[0.005, 0.1]
Cold Dark Matter Density	$\Omega_c h^2$	[0.001, 0.99]
Angular Size of Acoustic Horizon	$100\theta_{\rm MC}$	[0.5, 10.0]
Optical Depth	τ	[0.01, 0.8]
Scalar Spectral Index	n_s	[0.8, 1.2]
Scalar Amplitude	$\ln(10^{10}A_s)$	[2, 4]
Anisotropic Spectral Index	α	[0, 8]
Anisotropic Amplitude	B_0	[-1, 1]

Table 3 The Best-fit Parameter Values with 1σ Error Obtained from MCMC Analysis

Parameter	Best-fit (ΛCDM)	Best-fit (with power law form)	Best-fit (with exponential form)
$\Omega_b h^2$	0.02222 ± 0.00023	0.02037 ± 0.00021	0.01938 ± 0.00031
$\Omega_c h^2$	0.1197 ± 0.0022	0.1255 ± 0.0025	0.1430 ± 0.0053
$100\theta_{\rm MC}$	1.04085 ± 0.00047	1.03934 ± 0.00046	1.03789 ± 0.00059
τ	0.078 ± 0.019	0.057 ± 0.022	0.053 ± 0.020
n_s	0.9655 ± 0.0062	0.9365 ± 0.0081	0.9794 ± 0.0144
$\ln(10^{10}A_s)$	3.098 ± 0.036	3.067 ± 0.046	3.042 ± 0.037
α(model parameter)		0.4556 ± 0.2158	4.2889 ± 1.2173
B_0(model parameter)		0.04	0.4229 ± 0.1134

Notes: The first column presents the PLANCK 2015 best-fit ΛCDM parameter values, and the second and third columns list the parameter values for our theoretical model having power law and exponential forms of the anisotropic power spectrum respectively.

nential forms of the anisotropic power spectrum take $(B_0, \alpha) = (0.04, 0.4556 \pm 0.2185)$ and $(B_0, \alpha) = (0.4229 \pm 0.1134, 4.2889 \pm 1.2173)$ respectively. As we see from this figure, both forms of the anisotropic power spectrum are able to explain the lack of power for the multipole range $l = 2 - 10$. For the multipole range $l = 10 - 40$, our model fails to explain the observed lack of power. The power spectrum in our theoretical model also has some disagreement with the observed data at high-l which we neglect for the time being. The contour plots for both forms of the anisotropic power spectrum are shown in Figures 2 and 3 respectively.

Figures 2 and 3 show that our theoretical parameters have a very poor correlation with each other. If we check the best-fit parameters given in Table 3, then the correction to the isotropic primordial power spectrum due to the anisotropic power spectrum affects all the six ΛCDM parameters themselves. Out of these six ΛCDM parameters, five parameters differ by a small quantity from the PLANCK 2015 best-fit result whereas the τ parameter differs a lot. Hence to explain the lack of power spectrum throughout the observed multipole range $l = 2 - 40$, our theoretical model is not so efficient.

5 CONCLUSIONS

In this work, we have analyzed the direction dependent power spectrum obtained from Finsler space-time. Here we have considered up to the second order correction of the primordial power spectrum. The first order correction of the power spectrum produced the correlation between the multipoles that differs by $\Delta l = 1$, whereas the second order correction produced the correlation between the multipoles that differs by $\Delta l = 2$ in addition to the multipoles differing by $\Delta l = 0$. We found that the correlation between the multipoles differing by $\Delta l = 0$ has a contribution to the isotropic angular power spectrum C_l^{TT}. Here we are only interested in this correction term of the isotropic angular power spectrum and studied its effect on the observed low-l anomalies in the CMB data. We have explicitly studied the lack of power in the low multipole range $l \leq 40$. We have parameterized the anisotropic power spectrum $B(k)$ of the quadrupolar modulation term and applied the CosmoMC software to determine best-fit model parameters using the PLANCK likelihood code. We considered the power law as well as an exponential form of the anisotropic power spectrum.

For the power law form of the anisotropic spectrum, we found that for $B_0 = 0.04$ and $\alpha = 0.4556 \pm 0.2158$, our model is able to explain the lack of power in the multipole range $l = 2 - 10$. Whereas to explain the lack of power in the same multipole range, the exponential form of the anisotropic power spectrum took $\alpha = 4.2889 \pm 1.2173$ and $B_0 = 0.4229 \pm 0.1134$. But for the multipole range $l = 10 - 40$, our theoretical model approaches the ΛCDM result. Hence we found that our theoretical model could not explain the lack of power for the observed range of multipoles ($l = 2 - 40$) significantly. This may indicate a more complex form of the anisotropic model which could be able to explain all the low-l anomalies successfully.

Acknowledgements We acknowledge the use of CosmoMC software for our analysis. This work has been funded by the National Natural Science Foundation of China (Grant Nos. 11375203, 11675182 and 11690022).

References

Abramo, L. R., Bernui, A., Ferreira, I. S., Villela, T., & Wuensche, C. A. 2006a, Phys. Rev. D, 74, 063506

Abramo, L. R., Sodré, Jr., L., & Wuensche, C. A. 2006b, Phys. Rev. D, 74, 083515

Ackerman, L., Carroll, S. M., & Wise, M. B. 2007, Phys. Rev. D, 75, 083502

Aluri, P. K., & Jain, P. 2012, Modern Physics Letters A, 27, 1250014

Aluri, P. K., Ralston, J. P., & Weltman, A. 2017, MNRAS, 472, 2410

Bao, D., Chern, S.-S., & Shen, Z. 2012, An Introduction to Riemann-Finsler Geometry, 200 (Springer Science & Business Media)

Ben-David, A., Kovetz, E. D., & Itzhaki, N. 2012, ApJ, 748, 39

Bennett, C. L., Hill, R. S., Hinshaw, G., et al. 2011, ApJS, 192, 17

Berera, A., Buniy, R. V., & Kephart, T. W. 2004, J. Cosmol. Astropart. Phys., 10, 016

Boyanovsky, D., de Vega, H. J., & Sanchez, N. G. 2006, Phys. Rev. D, 74, 123006

Campanelli, L. 2009, Phys. Rev. D, 80, 063006

Chang, Z., Li, M.-H., Li, X., & Wang, S. 2013, European Physical Journal C, 73, 2459

Chang, Z., & Li, X. 2008, Physics Letters B, 663, 103

Chang, Z., & Li, X. 2009, Physics Letters B, 676, 173

Chang, Z., & Wang, S. 2012, European Physical Journal C, 72, 2165

Chang, Z., & Wang, S. 2013, European Physical Journal C, 73, 2516

Chang, Z., Wang, S., & Li, X. 2012, European Physical Journal C, 72, 1838

Cicoli, M., Downes, S., Dutta, B., Pedro, F. G., & Westphal, A. 2014, J. Cosmol. Astropart. Phys., 12, 030

Cohen, A. G., & Glashow, S. L. 2006, Physical Review Letters, 97, 021601

Coleman, S., & Glashow, S. L. 1997, Physics Letters B, 405, 249

Coleman, S., & Glashow, S. L. 1999, Phys. Rev. D, 59, 116008

Contaldi, C. R., Peloso, M., Kofman, L., & Linde, A. 2003, J. Cosmol. Astropart. Phys., 7, 002

Copi, C. J., Huterer, D., Schwarz, D. J., & Starkman, G. D. 2009, MNRAS, 399, 295

Copi, C. J., Huterer, D., Schwarz, D. J., & Starkman, G. D. 2015a, MNRAS, 451, 2978

Copi, C. J., Huterer, D., Schwarz, D. J., & Starkman, G. D. 2015b, MNRAS, 449, 3458

Copi, C. J., Huterer, D., & Starkman, G. D. 2004, Phys. Rev. D, 70, 043515

Cruz, M., Martínez-González, E., Vielva, P., & Cayón, L. 2005, MNRAS, 356, 29

Cruz, M., Martínez-González, E., Vielva, P., et al. 2008, MNRAS, 390, 913

Cruz, M., Tucci, M., Martínez-González, E., & Vielva, P. 2006, MNRAS, 369, 57

Das, S., & Souradeep, T. 2014, J. Cosmol. Astropart. Phys., 2, 002

de Oliveira-Costa, A., Tegmark, M., Zaldarriaga, M., & Hamilton, A. 2004, Phys. Rev. D, 69, 063516

Donoghue, J. F., Dutta, K., & Ross, A. 2009, Phys. Rev. D, 80, 023526

Emir Gümrükçüoglu, A., Contaldi, C. R., & Peloso, M. 2007, J. Cosmol. Astropart. Phys., 11, 005

Erickcek, A. L., Carroll, S. M., & Kamionkowski, M. 2008a, Phys. Rev. D, 78, 083012

Erickcek, A. L., Kamionkowski, M., & Carroll, S. M. 2008b, Phys. Rev. D, 78, 123520

Eriksen, H. K., Banday, A. J., Górski, K. M., Hansen, F. K., & Lilje, P. B. 2007, ApJ, 660, L81

Eriksen, H. K., Hansen, F. K., Banday, A. J., Górski, K. M., & Lilje, P. B. 2004, ApJ, 605, 14

Ghosh, S., Kothari, R., Jain, P., & Rath, P. K. 2016, J. Cosmol. Astropart. Phys., 1, 046

Gibbons, G. W., Gomis, J., & Pope, C. N. 2007, Phys. Rev. D, 76, 081701

Goldwirth, D. S., & Piran, T. 1990, Physical Review Letters, 64, 2852

Groeneboom, N. E., Axelsson, M., Mota, D. F., & Koivisto, T. 2010, arXiv:1011.5353

Gruppuso, A., Finelli, F., Natoli, P., et al. 2011, MNRAS, 411, 1445
Hansen, F. K., Banday, A. J., Górski, K. M., Eriksen, H. K., & Lilje, P. B. 2009, ApJ, 704, 1448
Hanson, D., & Lewis, A. 2009, Phys. Rev. D, 80, 063004
Hazra, D. K., Shafieloo, A., & Souradeep, T. 2014, J. Cosmol. Astropart. Phys., 11, 011
Hoftuft, J., Eriksen, H. K., Banday, A. J., et al. 2009, ApJ, 699, 985
Iqbal, A., Prasad, J., Souradeep, T., & Malik, M. A. 2015, J. Cosmol. Astropart. Phys., 6, 014
Jain, P., & Rath, P. K. 2015, European Physical Journal C, 75, 113
Jing, Y.-P., & Fang, L.-Z. 1994, Physical Review Letters, 73, 1882
Kahniashvili, T., Lavrelashvili, G., & Ratra, B. 2008, Phys. Rev. D, 78, 063012
Kim, J., & Komatsu, E. 2013, Phys. Rev. D, 88, 101301
Kim, J., & Naselsky, P. 2010a, ApJ, 714, L265
Kim, J., & Naselsky, P. 2010b, Phys. Rev. D, 82, 063002
Kim, J., & Naselsky, P. 2011, ApJ, 739, 79
King, J. A., Webb, J. K., Murphy, M. T., et al. 2012, MNRAS, 422, 3370
Kothari, R., Ghosh, S., Rath, P. K., Kashyap, G., & Jain, P. 2016, MNRAS, 460, 1577
Land, K., & Magueijo, J. 2005, Physical Review Letters, 95, 071301
Lewis, A., & Challinor, A. 2002, Phys. Rev. D, 66, 023531
Lewis, A., Challinor, A., & Lasenby, A. 2000, ApJ, 538, 473
Li, X., & Chang, Z. 2010, Phys. Rev. D, 82, 124009
Li, X., & Chang, Z. 2012, Differential Geometry and its Applications, 30, 737
Li, X., & Chang, Z. 2014, Phys. Rev. D, 90, 064049
Li, X., & Lin, H.-N. 2017, Chinese Physics C, 41, 065102
Li, X., Lin, H.-N., Wang, S., & Chang, Z. 2015a, European Physical Journal C, 75, 181
Li, X., Wang, S., & Chang, Z. 2015b, European Physical Journal C, 75, 260
Lim, E. A., & Simon, D. 2012, J. Cosmol. Astropart. Phys., 1, 048
Moffat, J. W. 2005, J. Cosmol. Astropart. Phys., 10, 012
Pereira, T. S., Pitrou, C., & Uzan, J.-P. 2007, J. Cosmol. Astropart. Phys., 9, 006
Planck Collaboration, Ade, P. A. R., Aghanim, N., et al. 2014a, Astronomy and Astrophysics, 571, A15
Planck Collaboration, Ade, P. A. R., Aghanim, N., et al. 2014b, Astronomy and Astrophysics, 571, A16
Planck Collaboration, Aghanim, N., Arnaud, M., et al. 2016a, Astronomy and Astrophysics, 594, A11
Planck Collaboration, Ade, P. A. R., Aghanim, N., et al. 2016b, Astronomy and Astrophysics, 594, A16
Planck Collaboration, Ade, P. A. R., Aghanim, N., et al. 2016c, Astronomy and Astrophysics, 594, A17
Pontzen, A., & Challinor, A. 2007, MNRAS, 380, 1387
Pullen, A. R., & Kamionkowski, M. 2007, Phys. Rev. D, 76, 103529
Ralston, J. P., & Jain, P. 2004, International Journal of Modern Physics D, 13, 1857
Randers, G. 1941, Physical Review, 59, 195
Rath, P. K., Aluri, P. K., & Jain, P. 2015, Phys. Rev. D, 91, 023515
Rath, P. K., & Jain, P. 2013, J. Cosmol. Astropart. Phys., 12, 014
Rath, P. K., Mudholkar, T., Jain, P., Aluri, P. K., & Panda, S. 2013, J. Cosmol. Astropart. Phys., 4, 007
Shiraishi, M., Liguori, M., & Fergusson, J. R. 2015, J. Cosmol. Astropart. Phys., 1, 007
Spergel, D. N., Verde, L., Peiris, H. V., et al. 2003, ApJS, 148, 175
Vielva, P. 2010, Advances in Astronomy, 2010, 592094
Watanabe, M.-A., Kanno, S., & Soda, J. 2009, Physical Review Letters, 102, 191302
Webb, J. K., King, J. A., Murphy, M. T., et al. 2011, Physical Review Letters, 107, 191101
Zhao, W. 2014, Phys. Rev. D, 89, 023010
Zibin, J. P., & Contreras, D. 2017, Phys. Rev. D, 95, 063011